

Selective innervation of NK1 receptor–lacking lamina I spinoparabrachial neurons by presumed nonpeptidergic A δ nociceptors in the rat



Najma Baseer^a, Abdullah S. Al-Baloushi^b, Masahiko Watanabe^c, Safa A.S. Shehab^{b,*}, Andrew J. Todd^{a,*}

^a Institute of Neuroscience and Psychology, College of Medical, Veterinary, and Life Sciences, University of Glasgow, Glasgow, UK

^b Department of Anatomy, College of Medicine and Health Sciences, United Arab Emirates University, Al Ain, United Arab Emirates

^c Department of Anatomy, Hokkaido University School of Medicine, Sapporo, Japan

Sponsorships or competing interests that may be relevant to content are disclosed at the end of this article.

ARTICLE INFO

Article history:

Received 27 May 2014

Received in revised form 20 July 2014

Accepted 19 August 2014

Keywords:

Cholera toxin B subunit

Dorsal horn

Lamina I projection neuron

Spinal cord

Transganglionic tracing

ABSTRACT

Fine myelinated (A δ) nociceptors are responsible for fast, well-localised pain, but relatively little is known about their postsynaptic targets in the spinal cord, and therefore about their roles in the neuronal circuits that process nociceptive information. Here we show that transganglionically transported cholera toxin B subunit (CTb) labels a distinct set of afferents in lamina I that are likely to correspond to A δ nociceptors, and that most of these lack neuropeptides. The vast majority of lamina I projection neurons that received retrogradely labelled from the lateral parabrachial area, and these can be divided into 2 major groups based on expression of the neurokinin 1 receptor (NK1r). We show that CTb-labelled afferents form contacts on 43% of the spinoparabrachial lamina I neurons that lack the NK1r, but on a significantly smaller proportion (26%) of those that express the receptor. We also confirm with electron microscopy that these contacts are associated with synapses. Among the spinoparabrachial neurons that received contacts from CTb-labelled axons, contact density was considerably higher on NK1r-lacking cells than on those with the NK1r. By comparing the density of CTb contacts with those from other types of glutamatergic bouton, we estimate that nonpeptidergic A δ nociceptors may provide over half of the excitatory synapses on some NK1r-lacking spinoparabrachial cells. These results provide further evidence that synaptic inputs to dorsal horn projection neurons are organised in a specific way. Taken together with previous studies, they suggest that both NK1r⁺ and NK1r-lacking lamina I projection neurons are directly innervated by A δ nociceptive afferents.

© 2014 The Authors. Published by Elsevier B.V. on behalf of International Association for the Study of Pain. This is an open access article under the CC BY license (<http://creativecommons.org/licenses/by/3.0/>).

1. Introduction

Myelinated nociceptive primary afferents, most of which conduct in the A δ range, convey information that is perceived as fast pain [41]. Although some myelinated (A β /A δ) nociceptors have axons that extend throughout laminae I–V, many A δ nociceptors arborise mainly in lamina I of the dorsal horn [29,67,68], a region that contains a high density of projection neurons, nearly all of

which can be retrogradely labelled from the lateral parabrachial area [1,38,57].

Although virtually all lamina I projection neurons in rat respond to noxious stimuli [3,7,21], anatomical studies have identified specific populations that differ in their synaptic inputs. The majority (75% to 80%) of the projection cells express the neurokinin 1 receptor (NK1r), and these cells are densely innervated by peptidergic primary afferents, which are thought to provide approximately half of their excitatory synapses [36,60]. We have identified a small but distinctive population of giant projection neurons in lamina I that lack the NK1r. These cells are densely innervated by both excitatory and inhibitory interneurons, but seem to receive little (if any) direct primary afferent input [35,40]. Virtually nothing is known about the synaptic inputs to the remaining (NK1r-lacking) projection neurons in this lamina, although it has been shown that they receive a lower density of contacts from peptidergic primary

* Corresponding authors. Addresses: Department of Anatomy, College of Medicine and Health Sciences, United Arab Emirates University, PO Box 17666, Al Ain, United Arab Emirates. Tel.: +971 3 7137492; fax: +971 3 7672033 (S.A.S. Shehab). Spinal Cord Group, West Medical Building, University of Glasgow, University Avenue, Glasgow G12 8QQ, UK. Tel.: +44 141 330 5868; fax: +44 141 330 2868 (A.J. Todd).

E-mail addresses: s.shehab@uaeu.ac.ae (S.A.S. Shehab), andrew.todd@glasgow.ac.uk (A.J. Todd).

afferents than the NK1^r projection neurons [60]. It also has been reported that some of these cells can express NK1r de novo after peripheral nerve injury [47].

Cholera toxin B subunit (CTb) binds to the GM1 ganglioside, and when injected into intact somatic peripheral nerves, it is taken up and transported mainly by myelinated primary afferents. This results in labelling of axonal boutons in lamina I and in a region of the dorsal horn that extends ventrally from the inner half of lamina II (Ili) [17,23,43,49,69]. The labelling in lamina I is thought to correspond to central terminals of myelinated nociceptors, in particular those with A δ axons, whereas that in deeper laminae is mainly in low-threshold mechanoreceptive A δ and A β afferents [23,29,43].

Lamina I projection neurons are known to respond to activity in A δ afferents [7], and it has been reported that for at least some cells this is mediated through monosynaptic inputs [4,63,64]. However, the postsynaptic targets of CTb-labelled (presumed myelinated nociceptive) afferents in lamina I apparently have not been identified. The main aim of this study therefore was to test the hypothesis that these afferents are presynaptic to projection neurons in this lamina, and to determine whether such inputs preferentially target specific types of projection cell. Some A δ nociceptors express the neuropeptides calcitonin gene-related peptide (CGRP) and substance P, and these differ in their receptive field properties from A δ nociceptors that lack these peptides [25,26]. However, a preliminary immunofluorescence study suggested that there was little or no transport of CTb by peptidergic afferents [42]. We therefore tested whether CGRP or substance P were present in CTb-labelled boutons in lamina I and related this to expression of the vesicular glutamate transporter VGLUT2, which has been found in approximately 80% of these boutons [58].

2. Methods

2.1. Animals and tissue processing

All experiments were approved by the Animal Ethics Committee of the College of Medicine and Health Science of the United Arab Emirates University and were performed in accordance with the guidelines of the European Communities Council directive of 24 November 1986 (86/609/EEC).

Nine adult male Wistar rats (240 to 255 g; UAE University) were used in this study. All animals were anaesthetised with ketamine and xylazine (25 mg and 5 mg intramuscularly, respectively) and received an injection of 2 μ L of 1% or 2% CTb into the left sciatic nerve, as described previously [51]. Six of the rats were placed in a stereotaxic frame immediately after the nerve injection, and these animals received an injection of 50 nl 4% Fluorogold targeted on the lateral parabrachial area (LPb), to label spinoparabrachial

neurons [59]. Because the majority of lamina I spinoparabrachial neurons project contralaterally, the Fluorogold injection was targeted on the LPb on the right side. The animals made an uneventful recovery from general anaesthesia. Three days after the injections, they were terminally anaesthetised with urethane (625 mg intraperitoneally) and perfused with fixative containing 4% freshly depolymerised formaldehyde through the left cardiac ventricle. The L4 spinal segments of all rats and the brains of those that had received stereotaxic injections were removed and post-fixed for 4 hours. The brains were cut into 100- μ m coronal sections with a freezing microtome, and these were used to assess the spread of Fluorogold. The spinal cord segments were cut into transverse or horizontal sections (60 μ m thick) with a vibrating microtome and processed as described later.

2.2. Neurochemical analysis of CTb-labelled boutons in lamina I

Transverse spinal cord sections from the 3 rats that received only sciatic nerve injections were incubated for 3 days with goat anti-CTb, rabbit anti-VGLUT2, rat anti-substance P, and guinea pig anti-CGRP. Details of the sources and dilutions of the primary antibodies are given in Table 1. The sections were then incubated overnight in species-specific secondary antibodies raised in donkey and conjugated to Alexa 488 (Life Technologies) or to Rhodamine Red, DyLight 649, or biotin (Jackson Immunoresearch). All secondary antibodies were diluted 1:500, apart from those conjugated to Rhodamine Red, which were diluted 1:100. The biotinylated antibody was revealed with Pacific Blue conjugated to avidin (1:1000; Life Technologies). Sections were mounted in antifade medium and stored at -20° C. All antibodies used in this part of the study were diluted in phosphate-buffered saline that contained 0.3% Triton X-100, and incubations were at 4° C.

Three sections were selected from each rat and scanned with a Zeiss LSM 710 confocal microscope (with Argon multiline, 405 nm diode, 561 nm solid-state and 633 nm HeNe lasers) through a 63 \times oil-immersion lens (NA 1.4) and a pinhole of 1 Airy unit. Several overlapping z-stacks (20 optical sections at 0.5 μ m z-separation) were scanned so as to include the whole of lamina I on the left side. Sections were analysed with NeuroLucida for Confocal software (MicroBrightField), and from each section, 100 CTb-immunoreactive boutons were selected from across the full mediolateral extent of CTb labelling in lamina I. This selection was made before other channels were viewed. The remaining channels were then switched on and the neurochemical phenotype of each of the selected CTb boutons was assessed. In order to determine whether variations in the sizes of different types of bouton could have resulted in a sampling bias, we measured the z-axis lengths of a sample of boutons of each of the major neurochemical types by determining the number of optical sections on which they appeared and multiplying this by 0.5 μ m (the z-spacing) [48].

2.3. Contacts between CTb-labelled A δ afferents and lamina I spinoparabrachial neurons

Horizontal sections of spinal cord from 4 of the rats that received sciatic and LPb injections were incubated in mouse anti-CTb, rabbit anti-NK1r, goat anti-VGLUT2, and guinea pig anti-Fluorogold, which were revealed with fluorescent secondary antibodies as described earlier. In order to estimate the proportion of projection neurons with or without the NK1r that received contacts from CTb-labelled A δ afferents, 1 or 2 horizontal sections that contained the largest number of lamina I projection neurons were selected from each rat and scanned through the 40 \times objective lens (NA 1.3) with a z-step of 1 μ m. A set of overlapping fields was scanned to include the entire mediolateral and rostrocaudal extent of lamina I on the left side within each of these sections. All retrogradely labelled cells,

Table 1
Primary antibodies used in this study.

Antibody	Species	Catalogue number	Dilution	Source
CTb	Goat	703	1:5000	List biological
CTb	Mouse	ab35988	1:5000	Abcam
VGLUT2	Goat		1:500	M. Watanabe
VGLUT2	Rabbit	135 402	1:5000	Synaptic systems
CGRP	Guinea pig	T-5027	1:10,000	Bachem
Substance P	Rat	OBT06435	1:200	Oxford biotech
NK1r	Rabbit	S8305	1:10,000	Sigma Aldrich
Fluorogold	Guinea pig	NM101	1:500	Protos biotech

apart from those that had substantial parts of the soma or dendritic tree missing from the section, were identified and classified into 1 of 3 types: (1) NK1r-immunoreactive cells (NK1r⁺), (2) giant cells (identified by the high density of VGLUT2 boutons on their cell bodies and proximal dendrites [35]), and (3) projection neurons that were not giant cells and that lacked the NK1r (NK1r-lacking cells). For each cell, the dendritic tree was followed as far as possible through the z-stack and the presence or absence of contacts from CTb-labelled boutons was recorded.

Examination of these sections revealed that relatively few NK1r⁺ projection cells received contacts from CTb boutons, and these contacts were generally at a low density. In contrast, a higher proportion of NK1r-lacking projection cells were contacted by CTb boutons, and these contacts were more numerous. We therefore carried out a detailed analysis of contact density on a sample of NK1r-lacking and NK1r⁺ projection neurons. Because the degree of CTb labelling can vary among experiments, presumably reflecting differences in the numbers of axons that have taken up the injected tracer, we did not use a random sampling approach to select projection neurons for this analysis. Instead, we selected 20 Fluorogold-labelled NK1r-lacking lamina I cells (4 to 6 from each rat) and 18 Fluorogold-labelled NK1r⁺ cells (3 to 8 cells from each rat) that were seen to receive relatively high numbers of contacts, and scanned the cell bodies and as much of the dendritic tree as was visible within the section. The scans were obtained through the 63× oil-immersion lens to generate z-stacks with a z-separation of 0.5 μm. For both populations of cells, we used Neurolucida for Confocal to plot the locations of boutons in contact with the soma and dendrites of each cell that were CTb- and/or VGLUT2-immunoreactive. Because we found that a few CTb-labelled boutons in lamina I were CGRP-immunoreactive (see Results), we then re-incubated the sections with guinea pig anti-CGRP, revealed this with Pacific blue (the same fluorochrome as had been used to reveal Fluorogold), and rescanned the cells, as described earlier. Although both Fluorogold and CGRP were now labelled with Pacific blue, they could easily be discriminated by comparison with the initial scans, which did not show CGRP immunoreactivity [6]. All CTb boutons contacting the cells were re-examined to determine whether or not they contained CGRP. In addition, the locations of contacts that the cells received from CGRP-immunoreactive boutons that lacked CTb were plotted. Cell body surface areas were measured, and the surface areas of dendrites were estimated from their lengths and diameters, based on the assumption that they were cylindrical [6,60]. For all types of contact, the density per 1000 μm² of combined somatic and dendritic surface was determined.

2.4. Combined confocal and electron microscopy

To confirm that contacts between CTb-labelled afferents and spinoparabrachial neurons were associated with synapses, we used a combined confocal and electron microscopic technique [6,33,56]. In preliminary studies we found that CTb was highly sensitive to glutaraldehyde fixation, and in particular CTb immunoreactivity in lamina I was not detected even with very low concentrations of glutaraldehyde in the primary fixative. For this reason we carried out this part of the study on tissue from animals that had been perfusion-fixed with 4% formaldehyde (ie, without glutaraldehyde).

Horizontal sections of spinal cord from 2 rats that had received injections of CTb into the sciatic nerve and Fluorogold into the contralateral LPb were reacted with goat anti-CTb, rabbit anti-NK1r, and guinea pig anti-Fluorogold. The reaction was performed as described earlier, except that: (a) Triton was omitted, (b) the secondary antibody cocktail contained both biotinylated and fluorescent-labelled anti-goat antibodies, and (c) the sections were

incubated in avidin conjugated to horseradish peroxidase (HRP; 1:1000; Sigma) before being mounted and scanned [6,33,35].

Three retrogradely labelled neurons on the left side (2 NK1r-lacking cells from different animals, and 1 NK1r⁺ cell) that received contacts from CTb axons were selected and scanned. Low magnification confocal z-stacks were obtained to allow subsequent identification of the cells during the preparation of tissue for electron microscopy. High-magnification z-series were scanned with the 63× oil-immersion objective (z-step 0.5 μm) through the cell bodies and dendritic trees of each of these cells, and the locations of contacts that the cells received from CTb-immunoreactive boutons were noted. The sections containing these cells were further fixed with 1% glutaraldehyde in PB overnight. They were then reacted with 3,3'-diaminobenzidine (DAB) in the presence of hydrogen peroxide [6,33,35] to reveal CTb. The sections were osmicated, block-stained with uranyl acetate, and embedded in resin. The regions containing the selected cells were identified from the distribution of DAB, which could be correlated with the CTb immunoreactivity seen in the confocal images. The sections were mounted on blocks of cured resin and trimmed to the appropriate area. Series of ultrathin sections were cut through the cells with a diamond knife and collected in serial order on Formvar-coated single-slot grids. These were contrasted with lead citrate and viewed with a Philips CM 100 electron microscope. CTb-immunoreactive boutons could be identified by their DAB reaction product, whereas the dendrites of the selected projection neurons were recognised by their position in relation to these boutons.

2.5. Antibody characterisation

Specificity of the CTb and Fluorogold antibodies is shown by lack of staining in regions that did not contain transported tracer. The goat and rabbit VGLUT2 antibodies were raised against amino acids 550 to 582 of rat VGLUT2 and 510 to 582 of mouse VGLUT2, respectively, and both recognise a single protein band of the appropriate molecular weight [20,55]. The CGRP antibody detects both α and β forms of the peptide. The monoclonal substance P antibody detects the C-terminal 5 to 8 amino acids of the peptide [10], and does not seem to recognise neurokinin B [37]. The NK1r antibody, raised against amino acids 393–407 of the rat NK1r, recognises a 46 kDa band in Western blots of rat brain extracts, and it has been shown that there is no staining with this antibody in mice in which the NK1r has been deleted [39].

2.6. Statistics

One-way ANOVA was used to test for differences in the z-axis lengths of different neurochemical types of CTb-labelled bouton in lamina I. A Student *t* test was used to determine whether there was a significant difference in the proportions of NK1r⁺ and NK1r-lacking projection neurons that received contacts from CTb-labelled boutons. Mann-Whitney *U* tests were used to compare densities of contacts from different types of axonal bouton onto these 2 different populations of projection neurons.

3. Results

3.1. VGLUT2 and neuropeptide expression by CTb boutons in lamina I

After injection of CTb into the sciatic nerve, CTb-immunoreactive boutons were densely distributed throughout the sciatic territory in the deep part of the dorsal horn, extending ventrally from lamina III, and in addition there was a sparser plexus of labelled boutons in lamina I in the corresponding region, as described in several previous studies [23,43,49–51,58,69] (Fig. 1a). The

distribution of staining for VGLUT2, CGRP, and substance P was the same as that described previously [2,15,16,24,34,58], and in all cases immunostaining was detected throughout the full thickness of the sections.

Consistent with our previous report [58], we found that the majority of CTb-labelled boutons in lamina I (mean 75%; Table 2) were VGLUT2-immunoreactive, although the strength of immunostaining varied considerably between boutons. Because some A δ nociceptors are peptidergic [25,26], and many peptidergic primary afferent terminals in the dorsal horn do not have detectable levels of VGLUT2 [24,32,58], we tested whether the CTb⁺/VGLUT2⁻ boutons in lamina I corresponded to peptidergic terminals. Although numerous boutons containing CGRP were observed in lamina I, only 11.4% of the CTb boutons in this lamina showed CGRP immunoreactivity, and most of these (75.9%) were also VGLUT2⁺ (Table 2, Fig. 1b to e). The remaining 24.1% of CGRP⁺ boutons (ie, those that lacked VGLUT2) constituted 2.7% of all CTb-labelled boutons (24.1% of 11.4%), and therefore accounted for only about 10% of the CTb boutons that lacked VGLUT2. Substance P was found in an even lower proportion of CTb-labelled boutons (mean 2.3%), and all of these were CGRP-immunoreactive (Fig. 1e inset). The mean z-axis lengths of nonpeptidergic CTb boutons with and without VGLUT2 was $2.72 \pm 0.65 \mu\text{m}$ and $2.69 \pm 0.54 \mu\text{m}$, respectively ($n = 40$ boutons in each case). The corresponding values for CTb boutons with CGRP but not substance P and for those with both peptides were $2.68 \pm 0.58 \mu\text{m}$ and $2.71 \pm 0.56 \mu\text{m}$, respectively ($n = 20$ boutons in each case). These values did not differ significantly (ANOVA, $P = 0.99$), indicating that our estimates of the proportion of each neurochemical type are unlikely to have been affected by sampling bias.

These results indicate that peptidergic afferents (particularly those that contain substance P) are seldom CTb-labelled, and can only account for a small proportion of the CTb⁺/VGLUT2⁻ boutons in lamina I. The discrepancy between our findings and those of Rivero-Melian et al. [42], who did not observe any colocalisation

Table 2
Neurochemistry of CTb boutons in lamina I.

Rat	VGLUT2 ⁺	CGRP ⁺	SP ⁺	VGLUT2 ⁺ /CGRP ⁺	CGRP ⁺ with VGLUT2
1	74	13.3	3.7	9.3	70
2	78.7	9.7	1.7	9	93.1
3	72.3	11.3	1.7	7.3	64.7
Mean	75	11.4	2.3	8.6	75.9

The second to fifth columns show the percentages of lamina I CTb boutons in each of the 3 rats that were immunoreactive for VGLUT2, CGRP, substance P, or both VGLUT2 and CGRP. The sixth column shows the percentage of CGRP⁺ CTb boutons that were also VGLUT2 immunoreactive.

of CTb with either CGRP or substance P, is probably explained by our use of confocal microscopy. This allows more accurate resolution of small profiles within a dense plexus of immunoreactive axons, as well as the detection of weakly labelled boutons.

3.2. Contacts between CTb boutons and lamina I projection neurons

In all cases, the Fluorogold injection site included the whole of the LPb, with variable spread into surrounding areas. An example is shown in Fig. 2. Quantitative data from the sections in which Fluorogold-labelled lamina I projection neurons were assessed for the presence or absence of contacts from CTb-immunoreactive primary afferent boutons are shown in Table 3. The mean number of projection neurons identified in each rat was 208, of which 71.6% were NK1r⁺, 2.1% were giant cells, and 26.3% were NK1r-lacking non-giant cells (defined as NK1r-lacking cells for convenience). As reported previously [35], we found that the giant cells did not receive contacts from CTb boutons. In contrast, 26.1% of the NK1r⁺ cells and 43.1% of the NK1r-lacking cells were found to receive contacts from CTb-labelled boutons. The proportions of neurons in these 2 populations that received contacts were significantly different ($P < .001$, t test).

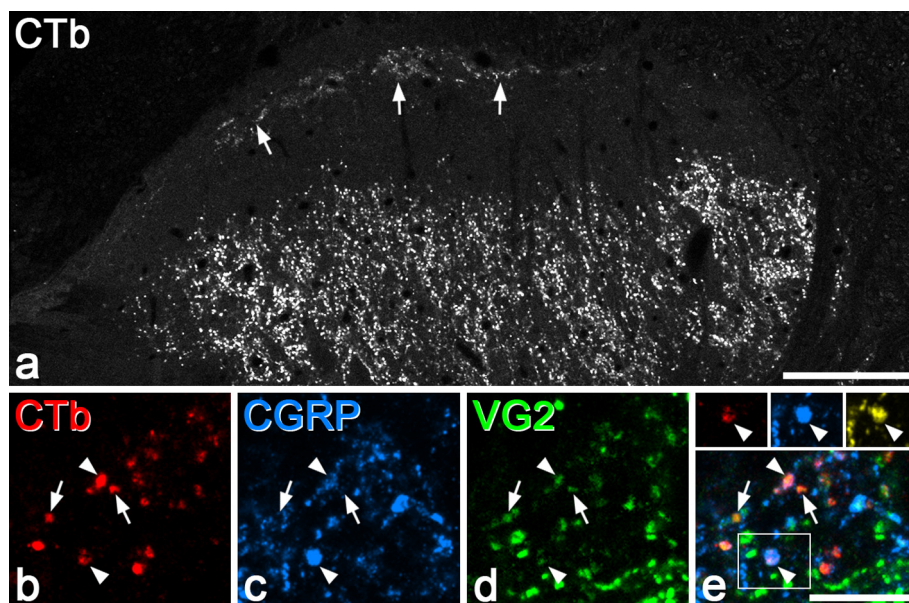


Fig. 1. Expression of neuropeptides and VGLUT2 by CTb-labelled primary afferents in lamina I. (a) Low-magnification view of the upper part of the dorsal horn showing the general distribution of CTb-labelled profiles seen in a transverse section. Arrows point to the plexus of labelled axons in lamina I, and below this there are very few labelled structures in the outer part of lamina II. (b–d) Confocal images from a section scanned to reveal (b) CTb (red), (c) CGRP (blue), and (d) VGLUT2 (VG2, green). A merged image is shown (e). Several CTb-immunoreactive boutons are visible. Two of these are CGRP⁺, and these are marked with arrowheads. Arrows indicate 2 CTb-immunoreactive boutons that lack CGRP. Although most of the CTb-labelled boutons in this field contain VGLUT2, the level of expression of the transporter varies considerably between boutons. The inset in (e) (corresponding to the area in the box) shows the lower of the 2 CTb-labelled boutons that are marked with an arrowhead. This has been scanned to reveal CTb (red), CGRP (blue), and substance P (yellow), and the bouton can be seen to contain both peptides. (a) Projection of 2 optical sections at $1 \mu\text{m}$ z-separation. (b–e) Projection of 2 optical sections at $0.5 \mu\text{m}$ z-separation. Scale bars: (a) = $100 \mu\text{m}$, (b–e) = $10 \mu\text{m}$.

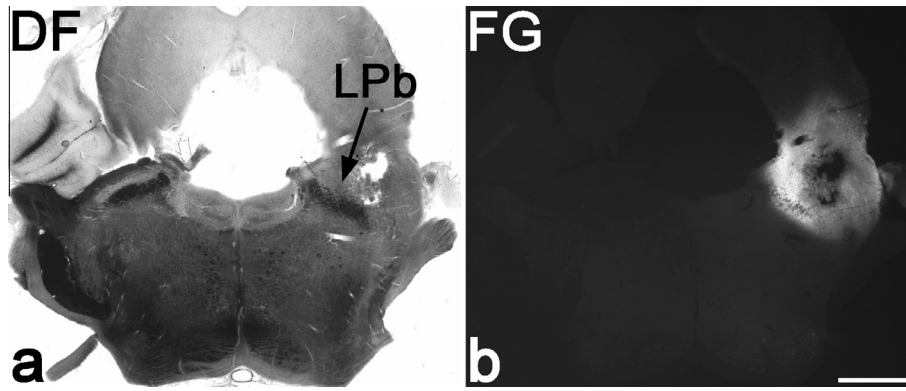


Fig. 2. Example of a Fluorogold injection site. (a, b) Dark field (DF) transmitted and fluorescent views of a section through the brainstem of one of the rats used in this study. The Fluorogold (FG) has spread throughout the entire lateral parabrachial area (LPb), with some extension into nearby structures. Scale bar = 1 mm.

Table 3
Analysis of contacts onto different types of projection neuron.

Rat	Total projection cells	NK1r ⁺ cells	Giant cells	NK1r-lacking cells	NK1r ⁺ cells with contacts (%)	NK1r-lacking cells with contacts (%)
1	254	183 (72%)	7 (2.8%)	64 (25.2%)	28	40.6
2	190	134 (70.5%)	3 (1.6%)	53 (27.9%)	26.9	47.2
3	200	128 (64%)	5 (2.5%)	67 (33.5%)	26.6	44.8
4	187	149 (80%)	3 (1.6%)	35 (18.7%)	22.8	40
Mean	207.8	148.5 (71.6%)	4.5 (2.1%)	54.8 (26.3%)	26.1	43.1

The second to fifth columns show the total numbers of projection neurons sampled and the number (percent) belonging to each class for the 4 rats from which sections were analysed. The last 2 columns show the percentage of cells of the corresponding type that received contacts from CTb-labelled boutons. No contacts were seen on the giant cells.

During this part of the study, we observed that those NK1r-lacking projection cells that received contacts from CTb-labelled boutons invariably had several such contacts, whereas for the NK1r⁺ projection cells contacted by CTb boutons, these contacts seemed to be far less numerous. This observation was confirmed by the quantitative analysis of contacts onto the 20 NK1r-lacking cells and 18 NK1r⁺ cells (Table 4, Figs. 3 and 4). The NK1r-lacking projection cells in this sample received a far higher density of contacts from CTb⁺ boutons (31.7/1000 μm²) than the NK1r⁺ projection cells (9.1/1000 μm²) ($P < .001$, Mann-Whitney *U* test). Virtually all (99.7%) of the CTb⁺ boutons in contact with the NK1r-lacking cells did not contain CGRP, whereas 7% of the CTb boutons that contacted the NK1r⁺ cells were CGRP-immunoreactive. However, the latter accounted for only 2% of all the CGRP boutons in contact with the NK1r⁺ cells. The contact densities for the CTb boutons that lacked CGRP are shown in Fig. 5, and this indicates that virtually all of the NK1r⁺ cells had a lower density in comparison to the NK1r-lacking cells.

In contrast, the densities of contacts from both the CGRP⁺ and VGLUT2⁺/CGRP⁻ boutons that lacked CTb were considerably higher on the NK1r⁺ cells (26.6 and 16.8/1000 μm², respectively) than on the NK1r-lacking cells (3.1 and 9.7/1000 μm²), and these differences were both significant ($P < .001$, Mann-Whitney *U* test).

Because the NK1r-immunostaining outlined the dendrites of NK1r⁺ projection neurons, these dendrites could be traced until they terminated or left the section. However, although Fluorogold filling allowed considerable lengths of dendrites of the NK1r-lacking projection cells to be identified, it is unlikely that these could be followed to their terminations, and therefore a greater proportion of distal dendrites will have been excluded from the analysis for the NK1r-lacking cells. If contacts were highly concentrated on the proximal dendrites of projection neurons, then the identification of more distal dendrites for the NK1r⁺ cells could have contributed to the difference in contact density that we observed for the CTb⁺/CGRP⁻ boutons. In order to test for this possibility, we performed a Sholl analysis, using shells with incremental

Table 4
Contact density on NK1r⁺ and NK1r-lacking projection neurons.

	CTb ⁺ /CGRP ⁻		CTb ⁺ /CGRP ⁺		CTb ⁻ /CGRP ⁺		CTb ⁻ /VGLUT2 ⁺ /CGRP ⁻	
	Number	Density	Number	Density	Number	Density	Number	Density
NK1r ⁺ (n = 18)	43.6 (14–145)	8.5 (2.8–24.3)	3.2 (0–7)	0.6 (0–1.5)	140.7 (62–266)	26.6 (16.7–43.1)	87.7 (23–137)	16.8 (9.3–31.8)
NK1r-lacking (n = 20)	79.9 (30–210)	31.6 (20.8–45.9)	0.2 (0–2)	0.1 (0–0.5)	7.5 (2–15)	3.1 (1.2–8)	26.5 (5–99)	9.7 (4–22.4)

The mean numbers of different neurochemical types of CTb-labelled bouton that contacted the 18 NK1r⁺ and 20 NK1r-lacking lamina I projection neurons, together with the density of contacts (per 1000 μm² of combined somatic and dendritic surface). Ranges are given in parentheses.

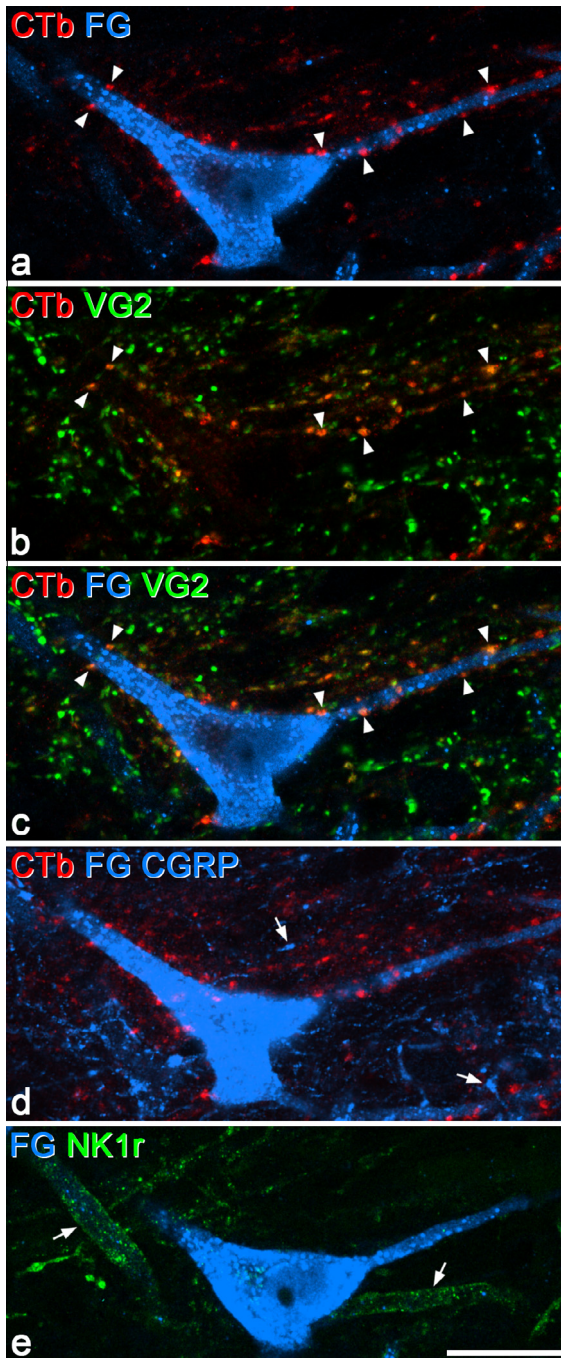


Fig. 3. A NK1r-lacking lamina I spinoparabrachial neuron that receives numerous contacts from CTb-labelled primary afferent boutons. Confocal images from a section reacted to reveal Fluorogold (FG), CTb, VGLUT2 (VG2), and the NK1r. (a–c) Projection of 3 optical sections at 0.5 μm z-separation through the cell body and proximal dendrites of a lamina I neuron retrogradely labelled with Fluorogold (blue), which receives numerous contacts from CTb-immunoreactive boutons (red), some of which are indicated with arrowheads. Several of these boutons are also labelled with the VGLUT2 antibody (green), and therefore appear orange in the merged images. The lamina I neuron received relatively few contacts from other VGLUT2⁺ boutons. (d) An equivalent projected image through the same section after it had been reacted to reveal CGRP (which appears in the same colour channel as Fluorogold). CGRP is represented by blue profiles that were not visible in (a), and 2 of these are indicated with arrows. Note that because the section was remounted before scanning, its orientation is not exactly the same as in (a–c), and therefore not all of the CTb-labelled profiles are visible. However, it is clear that none of those contacting the cell are CGRP-immunoreactive. (e) Projection of 3 different z-sections through the same cell to show the relationship between NK1r (green) and Fluorogold (blue). The retrogradely labelled cell lacks the receptor, but there are 2 nearby dendrites that are NK1r⁺ (arrows). Scale bar = 20 μm .

separations of 20 μm (Fig. 6). The results of this analysis showed that although contact density varied considerably within each projection neuron population, there was no sign of clustering of contacts on proximal dendrites for either population. It is therefore unlikely that a lower density of contacts from CTb⁺/CGRP⁻ boutons on distal dendrites of the NK1r⁺ projection neurons contributed to the lower overall contact density that was seen on these cells.

3.3. Combined confocal and electron microscopy

Although the ultrastructural preservation of the tissue was compromised by the lack of glutaraldehyde in the primary fixative, the CTb-labelled boutons and the dendrites of the selected projection neurons could easily be recognised (Fig. 7a and b), and synapses could be identified. We were able to find a total of 32 CTb⁺ boutons that were in contact with the 2 NK1r-lacking spinoparabrachial cells (19 on one cell and 13 on the other). In the great majority of cases (17 of 19 on the first cell and all 13 on the second cell), the bouton was seen to form an asymmetrical synapse with the projection neuron (Fig. 7c to f). Six CTb-labelled boutons in contact with the NK1r⁺ projection neuron were identified, and 5 of these were associated with an asymmetrical synapse (Fig. 7g).

4. Discussion

The main findings of this study are: (1) that the great majority of CTb-labelled sciatic afferents in lamina I are nonpeptidergic, and (2) that these afferents preferentially innervate a subset of NK1r-lacking projection neurons in this lamina.

4.1. CTb-labelling of presumed A δ nociceptors

Although CTb can be transported by unmyelinated visceral primary afferents [45,66] and axotomised somatic C fibres [50,62], several lines of evidence have led to the suggestion that transport by intact somatic afferents is largely restricted to those with myelinated axons [23,43,44,69]. Firstly, the great majority (94% to 97%) of neurons in the L5 dorsal root ganglion that bind CTb stain with the anti-neurofilament antibody RT97 [44,46], which has been used as a marker for cells with myelinated axons. Secondly, the laminar distribution of labelling after sciatic injection of CTb or CTb-HRP [23,42,49–51,69,70] matches that of myelinated primary afferents [8,28,29,52]. Thirdly, LaMotte et al. [23] showed that virtually all axons in the L4 dorsal root that contained CTb-HRP transported from the sciatic nerve were myelinated.

When CTb is injected into a chronically injured nerve, the pattern of central labelling changes and CTb-containing boutons appear in the outer part of lamina II (Ilo). This is thought to result from transport by axotomised C fibres that have upregulated the GM1 ganglioside [5,50,62]. Although it is possible that some C fibres were damaged by the sciatic nerve injections in our experiments, it is very unlikely that this would have resulted in CTb transport because the change in central labelling takes longer than 3 days after injury to develop [5,70]. Although we cannot rule out the possibility that the CTb in lamina I labels another population, such as thermoreceptors (which are thought to have unmyelinated axons in the rat [14,30]), it is highly likely that the CTb-labelled boutons that we observed in lamina I belong to myelinated nociceptive primary afferents, and specifically those with A δ axons [29,67,68].

4.2. Neuropeptides in A δ nociceptors

Electrophysiological recording from dorsal root ganglion cells in several species has demonstrated that many myelinated primary afferents express neuropeptides [22,25–27]. For example, Lawson

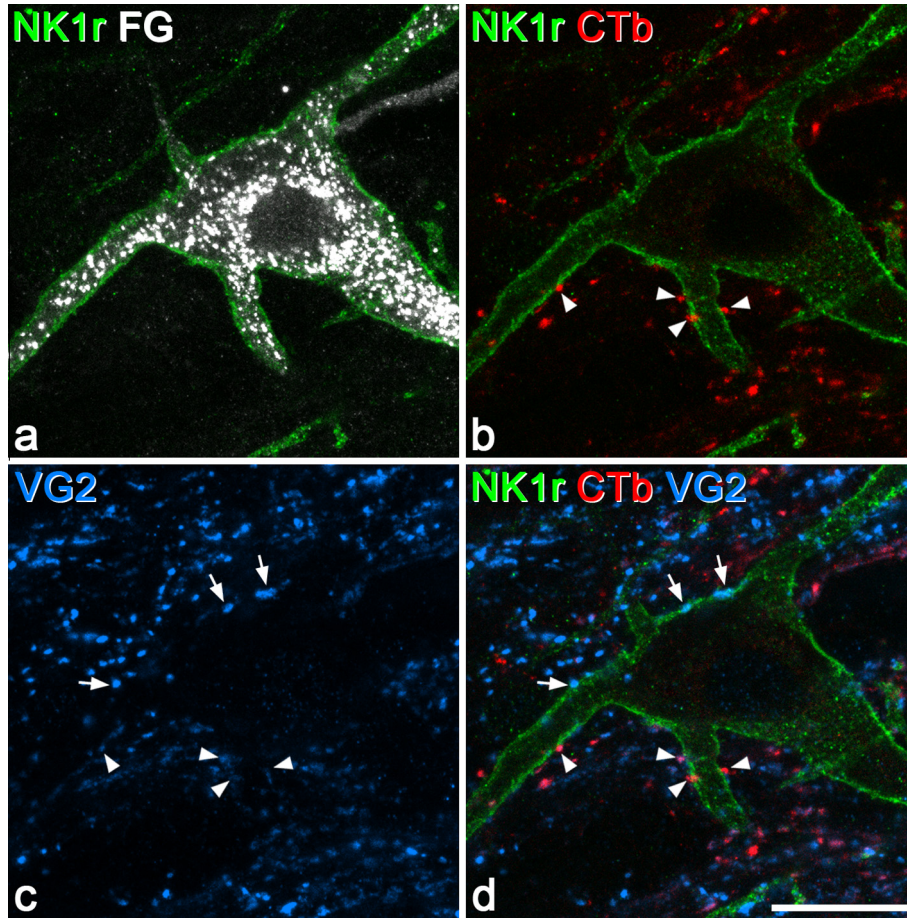


Fig. 4. A NK1r⁺ lamina I spinoparabrachial neuron that receives a few contacts from CTb-labelled boutons. (a–d) Combinations of staining for Fluorogold (FG, white), NK1r (green), CTb (red), and VGLUT2 (VG2, blue) in a projection of 6 optical sections (0.5 μm z-separation) through the cell body and proximal dendrites of a lamina I neuron labelled with Fluorogold from the lateral parabrachial area. The cell receives 4 contacts from CTb-labelled boutons (arrowheads), which show weak VGLUT2 immunoreactivity. It also receives several other contacts from VGLUT2-immunoreactive boutons, 3 of which are indicated with arrows. Scale bar = 20 μm.

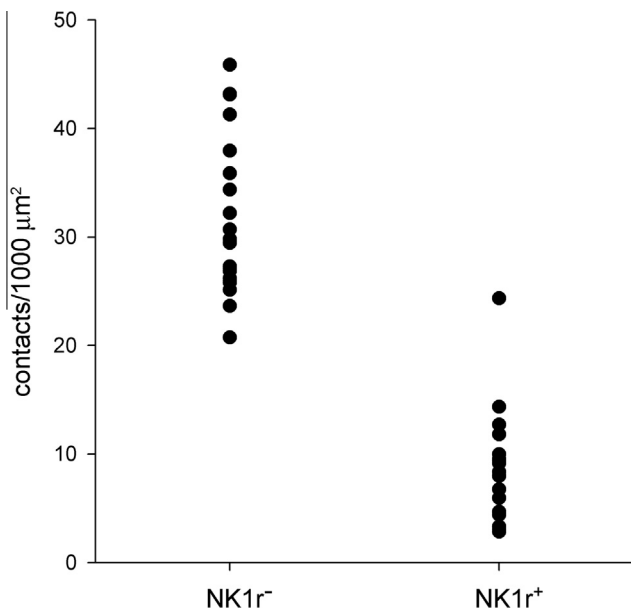


Fig. 5. Density of contacts from nonpeptidergic CTb-labelled boutons on projection neurons. A plot of the contact densities for CTb⁺ boutons that lacked CGRP onto projection neurons without (NK1r⁻, n = 20) and with (NK1r⁺, n = 18) the NK1 receptor. Density is expressed as the number of contacts from CTb⁺/CGRP⁻ boutons per 1000 μm² combined somatic and dendritic surface area.

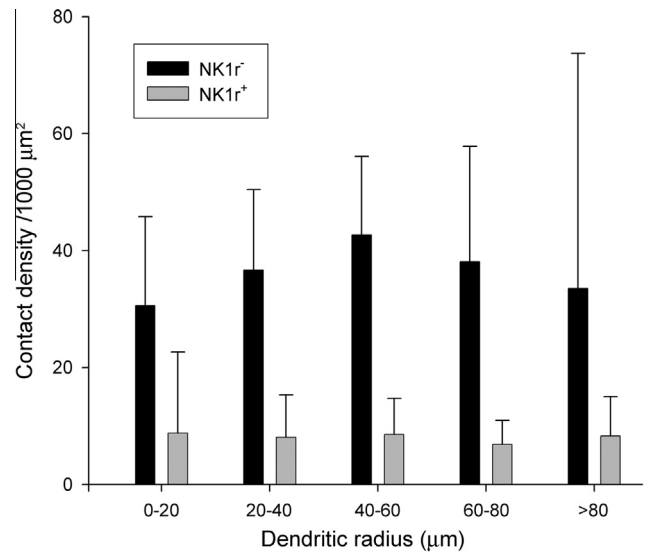


Fig. 6. Sholl analysis of the contact densities of nonpeptidergic CTb-labelled boutons on dendrites of projection neurons. The mean densities (\pm standard deviation) of contacts from CTb⁺/CGRP⁻ boutons on cells without (NK1r⁻, n = 20) or with (NK1r⁺, n = 18) the NK1 receptor. For each cell, 20-μm shells were centred on the midpoint of the soma and the contact density on dendrites occurring within each shell were measured. Note that although there is considerable variability within each shell, there is no clear trend toward either increasing or decreasing density with distance from the soma for either projection neuron population.

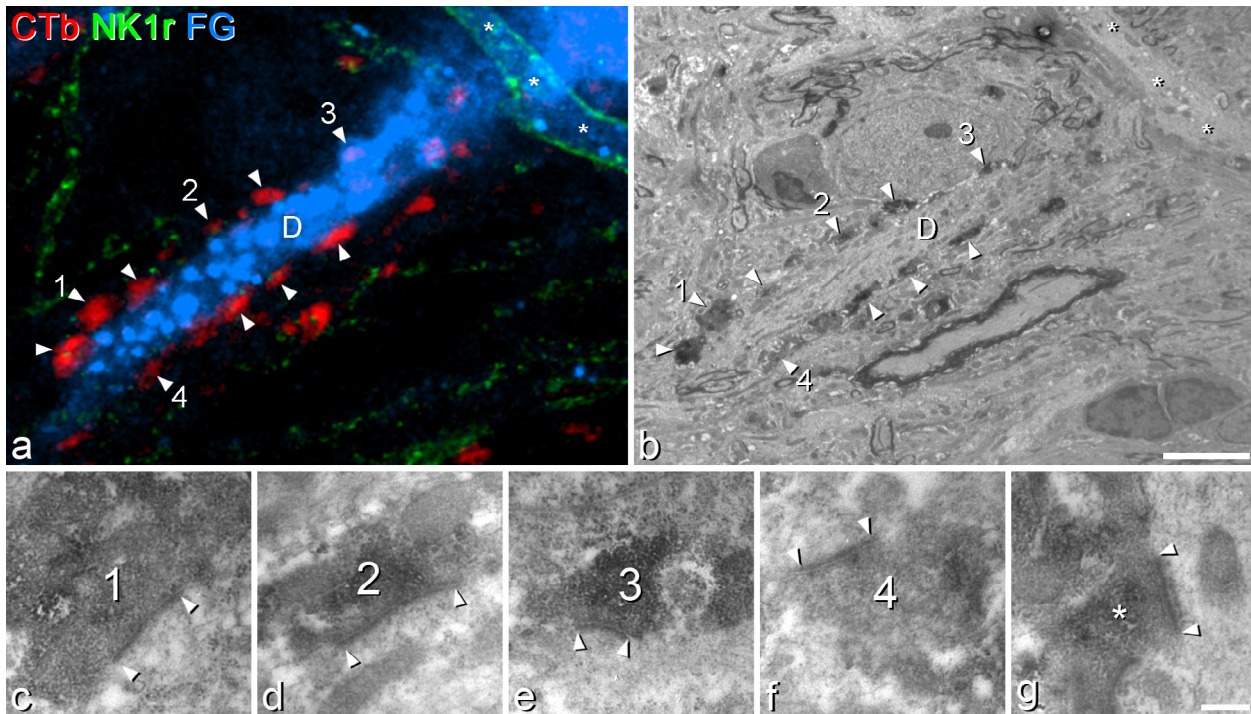


Fig. 7. Combined confocal and electron microscopy. (a) High-magnification confocal image (single optical section) through part of a dendrite [D] of one of the NK1r-lacking spinoparabrachial lamina I cells that was analysed with combined confocal and electron microscopy. It has been scanned to reveal CTb (red), NK1 receptor (green), and Fluorogold (FG, blue). The dendrite receives numerous contacts from CTb-labelled boutons (some marked with arrowheads). The numbers correspond to boutons that are illustrated in the high-magnification electron microscope (EM) images (c–f). Note that the bouton numbered 3 is partially obscured by Fluorogold in this confocal image. A small part of a dendrite belonging to a different spinoparabrachial cell is visible in the top right corner, and is indicated with asterisks. This cell expressed the NK1 receptor, which can be seen outlining the dendrite. (b) A low-magnification EM image of the region illustrated in (a), with corresponding structures marked. (c–f) High-magnification EM images of the 4 boutons indicated in (a) and (b). In each case, the synaptic specialisation is indicated (between arrowheads). (g) One of the synapses formed by a CTb-labelled bouton (*) onto a dendrite of the NK1r⁺ lamina I spinoparabrachial neuron that was analysed. Again, the synaptic specialisation is between the arrowheads. Scale bars: (b) = 5 μ m [also applies to (a)]; (g) = 0.5 μ m [also applies to (c–f)].

et al. reported that 5 of 12 A δ nociceptors in the guinea pig were CGRP-immunoreactive [25], whereas 8 of 16 contained substance P [26]. We have previously reported that approximately 20% of CTb-labelled boutons in lamina I lack detectable VGLUT2 [58], and because many peptidergic primary afferent boutons are not VGLUT2-immunoreactive [24,32,58], it was possible that the VGLUT2⁻/CTb⁺ boutons would correspond to peptidergic afferents. However, we found that only 11% of CTb-labelled afferents in lamina I contained CGRP, and most of these were VGLUT2-immunoreactive. Substance P was present in an even smaller proportion (2%) of the CTb-labelled boutons in this lamina.

Apart from species differences, there are 3 possible explanations for the discrepancy between the number of A δ nociceptors found to express neuropeptides in electrophysiological studies [25,26] and the low proportion of CTb-labelled peptidergic boutons seen in this study: (1) central terminals of peptidergic A δ nociceptors seldom terminate in lamina I, (2) the levels of neuropeptide in their central terminals are often undetectable, or (3) most of them do not transport CTb because they lack the GM1 ganglioside. The third explanation seems most likely because Robertson and Grant [44] reported that only 3% of L5 dorsal root ganglion cells that bound CTb were substance P-immunoreactive. This interpretation is also consistent with the finding by LaMotte et al. [23] that although most large myelinated axons in the L4 dorsal root were labelled after sciatic nerve injection of CTb-HRP, label was seen in a lower proportion of fine myelinated axons.

Lawson et al. [26] reported that substance P was present in most A δ nociceptors that responded to both noxious heat and mechanical stimulation, as well as those with deep receptive fields. However, none of the 20 A δ high-threshold mechanoreceptors

with superficial cutaneous receptive fields contained the peptide. It has since been suggested that many A δ fibres originally classified as A δ high-threshold mechanoreceptors [9] can respond to noxious heat, but with high thresholds (>53°C) and long latencies, and these have been classified as type I afferents [41,65]. The almost complete lack of coexistence of substance P and CTb seen in the present study suggests that the CTb-labelled boutons in lamina I may correspond to central terminals of type I A δ nociceptors.

4.3. Synaptic input from presumed A δ nociceptors to lamina I projection neurons

Between 75% and 80% of lamina I projection neurons express the NK1r [12,53,59], and these are densely innervated by substance P-containing primary afferents [60]. Around one fourth of these cells were found to receive contacts from CTb-labelled afferents, most of which were nonpeptidergic, and the electron microscopic results indicate that at least some of these are associated with synapses. However, the density of CTb contacts on these cells was relatively low compared with that of peptidergic afferents. Torsney and MacDermott have investigated primary afferent input to NK1r-expressing lamina I neurons, most of which were likely to be projection cells [63,64]. Around 30% of these received monosynaptic A δ input, presumably from A δ nociceptors. Interestingly, hindpaw inflammation increased the proportion of cells with monosynaptic A δ input to approximately 60%, and this was thought to reflect activation of previously silent synapses [63]. Although the A δ input seen in these experiments may have involved nonpeptidergic afferents, it is likely that some of the substance P⁺/CGRP⁺ boutons that synapse on NK1r-immunoreactive

projection neurons [60] belong to peptidergic A δ nociceptors, and that these contributed to the monosynaptic input.

Giant lamina I projection neurons have a highly characteristic pattern of inhibitory and excitatory synaptic input [35,40]. However, these cells are rare, accounting for approximately 3% of lamina I projection neurons. Therefore the remaining NK1r-lacking neurons constitute approximately 20% of the projection cells in this lamina. Until now, little was known about their synaptic inputs, but here we show that >40% of them receive contacts from presumed nonpeptidergic A δ nociceptors, that these contacts can be extremely numerous, and that they are associated with synapses.

Excitatory synapses in lamina I originate from local neurons, primary afferents, and descending axons [57]. The VGLUT2 antibody is likely to reveal the axons of all local excitatory neurons [58,71], as well as any descending axons, except for corticospinal axons, which are sparse in this lamina [13]. Apart from A δ nociceptors, most primary afferents in lamina I are peptidergic C fibres, which are CGRP-immunoreactive [19]. However, there is also a population of nonpeptidergic TRPM8⁺ thermoreceptive C fibres [11], and it is not yet known whether these express VGLUT2. It is therefore likely that most other glutamatergic boutons in lamina I (with the possible exception of TRPM8⁺ afferents) would be detected by the combination of CGRP and VGLUT2 antibodies used in this study. The mean density of contacts from CTb⁺/CGRP⁻ boutons on the 20 NK1r-lacking projection neurons was 32/1000 μm^2 , whereas the mean density of contacts from all other immunostained boutons (ie, those with CGRP and/or VGLUT2) was 13/1000 μm^2 (Table 4). For this group of NK1r-lacking projection cells, nonpeptidergic A δ (type I [41,65]) nociceptors could therefore provide up to 70% of their excitatory synapses, suggesting a very powerful synaptic input.

Two studies have tested responses of lamina I spinoparabrachial neurons to mechanical and thermal stimuli. All 53 cells recorded by Bester et al. [7] were activated by noxious heat, although with varying thresholds, and 92% responded to noxious mechanical stimuli. Andrew [3] also found that approximately 95% of spinoparabrachial neurons were driven by both noxious heat and mechanical stimuli. This indicates that the vast majority of lamina I spinoparabrachial neurons respond to noxious stimuli, and these presumably include most of the NK1r-lacking cells. Interestingly, a study using Fos as an activation marker [18] reported that NK1r-lacking lamina I projection neurons were significantly less likely to show Fos than those with the receptor after brief immersion of the foot in water at 52°C. This stimulus evoked Fos in 63% of NK1r⁺ lamina I spinoparabrachial cells, but only in 14% of those without the receptor [61]. The discrepancy between this result and the reports that virtually all spinoparabrachial lamina I cells respond to noxious heat [3,7] may be because nonpeptidergic A δ nociceptors with high heat thresholds (>53°C) [41,65] innervate many of the NK1r-lacking cells.

The finding that over 40% of NK1r-lacking spinoparabrachial cells are innervated by presumed A δ nociceptors suggests that these cells have an important role in perception of fast pain. Ablation of NK1r⁺ lamina I neurons with substance P-saporin reduced hyperalgesia in chronic pain states, but left acute pain thresholds intact [31,54]. Our findings suggest that synaptic input from A δ nociceptors to NK1r-lacking lamina I projection cells may have played a role in maintaining acute nociception in these animals.

These results provide further evidence that the primary afferent input to different types of projection neuron is organised in a specific way. This indicates that functional differences between nociceptor subtypes are, to some extent, maintained at the level of the projection neurons, which form the major output from the superficial dorsal horn.

Conflict of interest statement

The authors report no conflicts of interest.

Acknowledgements

The authors thank Mr. R. Kerr and Mrs. C. Watt for expert technical assistance. Financial support from the Wellcome Trust (grant number 102645), the Khyber Medical University, Pakistan, and the United Arab Emirates University (grant #31M070) is gratefully acknowledged.

References

- [1] Al-Khater KM, Todd AJ. Collateral projections of neurons in laminae I, III and IV of rat spinal cord to thalamus, periaqueductal grey matter and lateral parabrachial area. *J Comp Neurol* 2009;515:629–46.
- [2] Alvarez FJ, Villalba RM, Zerda R, Schneider SP. Vesicular glutamate transporters in the spinal cord, with special reference to sensory primary afferent synapses. *J Comp Neurol* 2004;472:257–80.
- [3] Andrew D. Sensitization of lamina I spinoparabrachial neurons parallels heat hyperalgesia in the chronic constriction injury model of neuropathic pain. *J Physiol* 2009;587:2005–17.
- [4] Andrew D. Quantitative characterization of low-threshold mechanoreceptor inputs to lamina I spinoparabrachial neurons in the rat. *J Physiol* 2010;588:117–24.
- [5] Bao L, Wang HF, Cai HJ, Tong YG, Jin SX, Lu YJ, Grant G, Hokfelt T, Zhang X. Peripheral axotomy induces only very limited sprouting of coarse myelinated afferents into inner lamina II of rat spinal cord. *Eur J Neurosci* 2002;16:175–85.
- [6] Baseer N, Polgar E, Watanabe M, Furuta T, Kaneko T, Todd AJ. Projection neurons in lamina III of the rat spinal cord are selectively innervated by local dynorphin-containing excitatory neurons. *J Neurosci* 2012;32:11854–63.
- [7] Bester H, Chapman V, Besson JM, Bernard JF. Physiological properties of the lamina I spinoparabrachial neurons in the rat. *J Neurophysiol* 2010;83:2239–59.
- [8] Brown AG, Fyffe RE, Rose PK, Snow PJ. Spinal cord collaterals from axons of type II slowly adapting units in the cat. *J Physiol* 1981;316:469–80.
- [9] Burgess PR, Perl ER. Myelinated afferent fibres responding specifically to noxious stimulation of the skin. *J Physiol* 1967;190:541–62.
- [10] Cuello AC, Galfre G, Milstein C. Detection of substance P in the central nervous system by a monoclonal antibody. *Proc Natl Acad Sci U S A* 1979;76:3532–6.
- [11] Dhaka A, Earley TJ, Watson J, Patapoutian A. Visualizing cold spots: TRPM8-expressing sensory neurons and their projections. *J Neurosci* 2008;28:566–75.
- [12] Ding YQ, Takada M, Shigemoto R, Mizumo N. Spinoparabrachial tract neurons showing substance P receptor-like immunoreactivity in the lumbar spinal cord of the rat. *Brain Res* 1995;674:336–40.
- [13] Du Beau A, Shakya Shrestha S, Bannatyne BA, Jalicy SM, Linnen S, Maxwell DJ. Neurotransmitter phenotypes of descending systems in the rat lumbar spinal cord. *Neuroscience* 2012;227:67–79.
- [14] Fleischer E, Handwerker HO, Joukhadar S. Unmyelinated nociceptive units in two skin areas of the rat. *Brain Res* 1983;267:81–92.
- [15] Gibson SJ, Polak JM, Bloom SR, Sabate IM, Mulderry PM, Ghatei MA, McGregor GP, Morrison JFB, Kelly JS, Evans RM, Rosenfeld MG. Calcitonin gene-related peptide immunoreactivity in the spinal cord of man and of 8 other species. *J Neurosci* 1984;4:3101–11.
- [16] Hokfelt T, Kellererth JO, Nilsson G, Pernow B. Substance-P – Localization in central nervous system and in some primary sensory neurons. *Science* 1975;190:889–90.
- [17] Hughes DI, Scott DT, Todd AJ, Riddell JS. Lack of evidence for sprouting of Abeta afferents into the superficial laminae of the spinal cord dorsal horn after nerve section. *J Neurosci* 2003;23:9491–9.
- [18] Hunt SP, Pini A, Evan G. Induction of c-fos-like protein in spinal cord neurons following sensory stimulation. *Nature* 1987;328:632–4.
- [19] Ju G, Hokfelt T, Brodin E, Fahrenkrug J, Fischer JA, Frey P, Elde RP, Brown JC. Primary sensory neurons of the rat showing calcitonin gene-related peptide immunoreactivity and their relation to substance P-, somatostatin-, galanin-, vasoactive intestinal polypeptide- and cholecystokinin-immunoreactive ganglion cells. *Cell Tissue Res* 1987;247:417–31.
- [20] Kawamura Y, Fukaya M, Maejima T, Yoshida T, Miura E, Watanabe M, Ohno-Shosaku T, Kano M. The CB1 cannabinoid receptor is the major cannabinoid receptor at excitatory presynaptic sites in the hippocampus and cerebellum. *J Neurosci* 2006;26:2991–3001.
- [21] Keller AF, Beggs S, Salter MW, De Koninck Y. Transformation of the output of spinal lamina I neurons after nerve injury and microglia stimulation underlying neuropathic pain. *Mol Pain* 2007;3:27.
- [22] Koerber HR, Woodbury CJ. Comprehensive phenotyping of sensory neurons using an ex vivo somatosensory system. *Physiol Behav* 2002;77:589–94.
- [23] LaMotte CC, Kapadia SE, Shapiro CM. Central projections of the sciatic, saphenous, median, and ulnar nerves of the rat demonstrated by transganglionic transport of cholera toxin B-subunit (B-HRP) and wheat germ agglutinin-HRP (WGA-HRP). *J Comp Neurol* 1991;311:546–62.

- [24] Landry M, Bouali-Benazzouz R, El Mestikawy S, Ravassard P, Nagy F. Expression of vesicular glutamate transporters in rat lumbar spinal cord, with a note on dorsal root ganglia. *J Comp Neurol* 2004;468:380–94.
- [25] Lawson SN, Crepps B, Perl ER. Calcitonin gene-related peptide immunoreactivity and afferent receptive properties of dorsal root ganglion neurones in guinea-pigs. *J Physiol* 2002;540:989–1002.
- [26] Lawson SN, Crepps BA, Perl ER. Relationship of substance P to afferent characteristics of dorsal root ganglion neurones in guinea-pig. *J Physiol* 1997;505:177–91.
- [27] Lawson SN, McCarthy PW, Prabhakar E. Electrophysiological properties of neurones with CGRP-like immunoreactivity in rat dorsal root ganglia. *J Comp Neurol* 1996;365:355–66.
- [28] Li L, Rutlin M, Abreira VE, Cassidy C, Kus L, Gong S, Jankowski MP, Luo W, Heintz N, Koerber HR, Woodbury CJ, Ginty DD. The functional organization of cutaneous low-threshold mechanosensory neurons. *Cell* 2011;147:1615–27.
- [29] Light AR, Perl ER. Spinal termination of functionally identified primary afferent neurons with slowly conducting myelinated fibers. *J Comp Neurol* 1979;186:133–50.
- [30] Lynn B, Carpenter SE. Primary afferent units from the hairy skin of the rat hind limb. *Brain Res* 1982;238:29–43.
- [31] Mantyh PW, Rogers SD, Honore P, Allen BJ, Ghilardi JR, Li J, Daughters RS, Lappi DA, Wiley RG, Simone DA. Inhibition of hyperalgesia by ablation of lamina I spinal neurons expressing the substance P receptor. *Science* 1997;278:275–9.
- [32] Morris JL, Konig P, Shimizu T, Jobling P, Gibbins IL. Most peptide-containing sensory neurons lack proteins for exocytotic release and vesicular transport of glutamate. *J Comp Neurol* 2005;483:1–16.
- [33] Naim M, Spike RC, Watt C, Shehab SA, Todd AJ. Cells in laminae III and IV of the rat spinal cord that possess the neurokinin-1 receptor and have dorsally directed dendrites receive a major synaptic input from tachykinin-containing primary afferents. *J Neurosci* 1997;17:5536–48.
- [34] Oliveira AL, Hydling F, Olsson E, Shi T, Edwards RH, Fujiyama F, Kaneko T, Hokfelt T, Cullheim S, Meister B. Cellular localization of three vesicular glutamate transporter mRNAs and proteins in rat spinal cord and dorsal root ganglia. *Synapse* 2003;50:117–29.
- [35] Polgár E, Al-Khater KM, Shehab S, Watanabe M, Todd AJ. Large projection neurons in lamina I of the rat spinal cord that lack the neurokinin 1 receptor are densely innervated by VGLUT2-containing axons and possess GluR4-containing AMPA receptors. *J Neurosci* 2008;28:13150–60.
- [36] Polgár E, Al Ghamdi KS, Todd AJ. Two populations of neurokinin 1 receptor-expressing projection neurons in lamina I of the rat spinal cord that differ in AMPA receptor subunit composition and density of excitatory synaptic input. *Neuroscience* 2010;167:1192–204.
- [37] Polgár E, Furuta T, Kaneko T, Todd A. Characterization of neurons that express preprotachykinin B in the dorsal horn of the rat spinal cord. *Neuroscience* 2006;139:687–97.
- [38] Polgár E, Wright LL, Todd AJ. A quantitative study of brainstem projections from lamina I neurons in the cervical and lumbar enlargement of the rat. *Brain Res* 2010;1308:58–67.
- [39] Ptak K, Burnet H, Bianchi B, Sieweke M, De Felipe C, Hunt SP, Monteau R, Hilaire G. The murine neurokinin NK1 receptor gene contributes to the adult hypoxic facilitation of ventilation. *Eur J Neurosci* 2002;16:2245–52.
- [40] Puskár Z, Polgár E, Todd AJ. A population of large lamina I projection neurons with selective inhibitory input in rat spinal cord. *Neuroscience* 2001;102:167–76.
- [41] Ringkamp M, Raja SN, Campbell JN, Meyer RA. Peripheral mechanisms of cutaneous nociception. In: McMahon S, Koltzenburg M, Tracey I, Turk DC, editors. *Wall and Melzack's textbook of pain*. Edinburgh: Elsevier; 2013. p. 1–30.
- [42] Rivero-Melian C, Rosario C, Grant G. Demonstration of transganglionically transported cholera toxin in rat spinal cord by immunofluorescence cytochemistry. *Neurosci Lett* 1992;145:114–7.
- [43] Robertson B, Grant G. A comparison between wheat germ agglutinin- and cholera toxin-horseradish peroxidase as anterogradely transported markers in central branches of primary sensory neurones in the rat with some observations in the cat. *Neuroscience* 1985;14:895–905.
- [44] Robertson B, Grant G. Immunocytochemical evidence for the localization of the GM1 ganglioside in carbonic anhydrase-containing and RT 97-immunoreactive rat primary sensory neurons. *J Neurocytol* 1989;18:77–86.
- [45] Robertson B, Lindh B, Aldskogius H. WGA-HRP and cholera toxin-HRP as anterogradely transported tracers in vagal visceral afferents and binding of WGA and cholera toxin to nodose ganglion neurons in rodents. *Brain Res* 1992;590:207–12.
- [46] Robertson B, Perry MJ, Lawson SN. Populations of rat spinal primary afferent neurons with cholera toxin binding compared with those labelled by markers for neurofilament and carbohydrate groups: a quantitative immunocytochemical study. *J Neurocytol* 1991;20:387–95.
- [47] Saeed AW, Ribeiro-da-Silva A. De novo expression of neurokinin-1 receptors by spinoparabrachial lamina I pyramidal neurons following a peripheral nerve lesion. *J Comp Neurol* 2013;521:1915–28.
- [48] Sardella TC, Polgar E, Watanabe M, Todd AJ. A quantitative study of neuronal nitric oxide synthase expression in laminae I–III of the rat spinal dorsal horn. *Neuroscience* 2011;192:708–20.
- [49] Shehab SA, Hughes DI. Simultaneous identification of unmyelinated and myelinated primary somatic afferents by co-injection of isolectin B4 and Cholera toxin subunit B into the sciatic nerve of the rat. *J Neurosci Methods* 2011;198:213–21.
- [50] Shehab SA, Spike RC, Todd AJ. Evidence against cholera toxin B subunit as a reliable tracer for sprouting of primary afferents following peripheral nerve injury. *Brain Res* 2003;964:218–27.
- [51] Shehab SA, Spike RC, Todd AJ. Do central terminals of intact myelinated primary afferents sprout into the superficial dorsal horn of rat spinal cord after injury to a neighboring peripheral nerve? *J Comp Neurol* 2004;474:427–37.
- [52] Shortland P, Woolf CJ, Fitzgerald M. Morphology and somatotopic organization of the central terminals of hindlimb hair follicle afferents in the rat lumbar spinal cord. *J Comp Neurol* 1989;289:416–33.
- [53] Spike RC, Puskár Z, Andrew D, Todd AJ. A quantitative and morphological study of projection neurons in lamina I of the rat lumbar spinal cord. *Eur J Neurosci* 2003;18:2433–48.
- [54] Suzuki R, Morcuende S, Webber M, Hunt SP, Dickenson AH. Superficial NK1-expressing neurons control spinal excitability through activation of descending pathways. *Nat Neurosci* 2002;5:1319–26.
- [55] Takamori S, Rhee JS, Rosenmund C, Jahn R. Identification of differentiation-associated brain-specific phosphate transporter as a second vesicular glutamate transporter (VGLUT2). *J Neurosci* 2001;21:RC182.
- [56] Todd AJ. A method for combining confocal and electron microscopic examination of sections processed for double- or triple-labelling immunocytochemistry. *J Neurosci Methods* 1997;73:149–57.
- [57] Todd AJ. Neuronal circuitry for pain processing in the dorsal horn. *Nat Rev Neurosci* 2010;11:823–36.
- [58] Todd AJ, Hughes DI, Polgar E, Nagy GG, Mackie M, Ottersen OP, Maxwell DJ. The expression of vesicular glutamate transporters VGLUT1 and VGLUT2 in neurochemically defined axonal populations in the rat spinal cord with emphasis on the dorsal horn. *Eur J Neurosci* 2003;17:13–27.
- [59] Todd AJ, McGill MM, Shehab SA. Neurokinin 1 receptor expression by neurons in laminae I, III and IV of the rat spinal dorsal horn that project to the brainstem. *Eur J Neurosci* 2000;12:689–700.
- [60] Todd AJ, Puskár Z, Spike RC, Hughes C, Watt C, Forrest L. Projection neurons in lamina I of rat spinal cord with the neurokinin 1 receptor are selectively innervated by substance P-containing afferents and respond to noxious stimulation. *J Neurosci* 2002;22:4103–13.
- [61] Todd AJ, Spike RC, Young S, Puskár Z. Fos induction in lamina I projection neurons in response to noxious thermal stimuli. *Neuroscience* 2005;131:209–17.
- [62] Tong YG, Wang HF, Ju G, Grant G, Hokfelt T, Zhang X. Increased uptake and transport of cholera toxin B-subunit in dorsal root ganglion neurons after peripheral axotomy: possible implications for sensory sprouting. *J Comp Neurol* 1999;404:143–58.
- [63] Torsney C. Inflammatory pain unmasks heterosynaptic facilitation in lamina I neurokinin 1 receptor-expressing neurons in rat spinal cord. *J Neurosci* 2011;31:5158–68.
- [64] Torsney C, MacDermott AB. Disinhibition opens the gate to pathological pain signaling in superficial neurokinin 1 receptor-expressing neurons in rat spinal cord. *J Neurosci* 2006;26:1833–43.
- [65] Treede RD, Meyer RA, Campbell JN. Myelinated mechanically insensitive afferents from monkey hairy skin: heat-response properties. *J Neurophysiol* 1998;80:1082–93.
- [66] Wang HF, Shortland P, Park MJ, Grant G. Retrograde and transganglionic transport of horseradish peroxidase-conjugated cholera toxin B subunit, wheatgerm agglutinin and isolectin B4 from *Griaffonia simplicifolia* I in primary afferent neurons innervating the rat urinary bladder. *Neuroscience* 1998;87:275–88.
- [67] Woodbury CJ, Koerber HR. Widespread projections from myelinated nociceptors throughout the substantia gelatinosa provide novel insights into neonatal hypersensitivity. *J Neurosci* 2003;23:601–10.
- [68] Woodbury CJ, Kullmann FA, McIlwraith SL, Koerber HR. Identity of myelinated cutaneous sensory neurons projecting to nociceptive laminae following nerve injury in adult mice. *J Comp Neurol* 2008;508:500–9.
- [69] Woolf CJ, Shortland P, Coggeshall RE. Peripheral nerve injury triggers central sprouting of myelinated afferents. *Nature* 1992;355:75–8.
- [70] Woolf CJ, Shortland P, Reynolds M, Ridings J, Doubell T, Coggeshall RE. Reorganization of central terminals of myelinated primary afferents in the rat dorsal horn following peripheral axotomy. *J Comp Neurol* 1995;360:121–34.
- [71] Yasaka T, Tiong SYX, Hughes DI, Riddell JS, Todd AJ. Populations of inhibitory and excitatory interneurons in lamina II of the adult rat spinal dorsal horn revealed by a combined electrophysiological and anatomical approach. *PAIN[®]* 2010;151:475–88.